

COLLOID RELEASE AND *E. COLI* TRANSPORT IN INTACT AGRICULTURAL SOIL COLUMNS

Gang Chen*, Kamal Tawfiq and Sandip Patil

Department of Civil Engineering and Environmental Engineering, FAMU-FSU College of Engineering, United States

Received 11 May 2012; received in revised form 14 October 2012; accepted 16 October 2012

Abstract:

During animal waste agricultural applications, the major concern is the pathogen spreading, which may contaminate groundwater. Colloid release and pathogen transport during irrigation were evaluated in intact agricultural soil columns in this research using *Escherichia coli* as a model strain. In order to be easily identified and quantified, *E. coli* was incorporated with green fluorescent protein genes. The experiments were conducted at a water flow rate of 100 ml/min and the elution was collected and analyzed for colloid release and *E. coli* transport. Colloid release and *E. coli* transport were simulated using an implicit, finite-difference scheme with colloid release rate coefficient and *E. coli* deposition rate coefficient as constant, linear and exponential functions of the soil depth, respectively. It seemed that exponential functions had the best fit against the colloid release and *E. coli* transport observations.

Keywords: Colloid release; *E. coli*; water content; irrigation.

© 2012 Journal of Urban and Environmental Engineering (JUEE). All rights reserved.

* Correspondence to: Gang Chen. E-mail: gchen@eng.fsu.edu.

INTRODUCTION

An increasing amount of animal waste is produced by intensive livestock operations, which accounts for two trillion pounds per year nationally (Hammond 1972; Haapapuro *et al.*, 1997; Krauss, 2003). Animal waste should be considered a valuable resource, which, when managed properly, can reduce the need for commercial synthesized fertilizer (Benckiser & Simarmata 1994). For instance, manure is commonly sprayed onto farm fields as fertilizer (Franco *et al.*, 2006).

Animal waste can add organic matter to improve the water holding capacity of the soil and tilth. It also provides an economical source of nitrogen, phosphorus and potassium as well as other nutrients needed for plant growth (Brannan *et al.*, 2000). However, animal waste is rich in infectious agents or pathogenic organisms, which include viruses, bacteria and pathogenic protozoa. The majority of these pathogens are enteric in origin which can cause waterborne diseases such as salmonellosis, typhoid fever, and cholera (by bacteria); viral gastroenteritis and hepatitis A (by viruses); and amoebic dysentery and cryptosporidiosis (by protozoa) through the fecal-oral route (Leclerc *et al.*, 2002; Gerba & Smith Jr., 2005; Al-Sa'ed, 2007; Yan & Sadowsky, 2007). Bacteria are the most common pathogenic microorganisms found in animal waste, among which *Salmonellae*, *Shigellae*, diarrheagenic *Escherichia coli* (including *E. coli* O157:H7), *Campylobacter* and *Vibrios* are of particular concern (McGarvey *et al.*, 2004; Gerba & Smith Jr., 2005). Viruses are also important and are potentially more infectious than bacteria. However, viruses are obligate intracellular parasites and are incapable of replication outside of host organisms, which are, in most cases, bacteria (Pesaro *et al.*, 1995). Common protozoa found in reclaimed wastewater are *Giardia* and *Cryptosporidium*, which are relatively large pathogenic microorganisms that can multiply only in the gastrointestinal tract of humans and other animals. They cannot multiply in the environment, but they can survive longer in water than intestinal bacteria and are more infectious and resistant to disinfection than most other microorganisms. Usually, the presence of *E. coli* is an indication that *Giardia* and *Cryptosporidium* could also be present (Schets *et al.*, 2008).

Thus, infectious agents or pathogenic organisms in the soil are usually symbolized by *E. coli*. Among the *E. coli* strains, *E. coli* O157:H7 is believed to be the most notorious pathogen. *Escherichia coli* O157:H7 produces a powerful toxin and can cause severe infection such as severe bloody diarrhea and abdominal cramps (Irina *et al.*, 2002). *Escherichia coli* O157:H7 mostly lives in the intestines of cattle, but has also been found in the

intestines of chickens, deer, sheep, and pigs (Jay *et al.*, 2007). *Escherichia coli* O157:H7 does not cause illness in animals, but the animals can serve as carriers for it. Infected animals, especially young ones, can shed the bacteria in their feces.

During animal waste land applications, there are concerns that infectious pathogenic organisms may spread in the subsurface soil with a possibility to contaminate the groundwater once these infectious pathogenic organisms pass through the vadose zone and reach the groundwater table (Brenner *et al.*, 1988). Special care must be taken to monitor their fate and transport during animal waste land applications (Walker *et al.*, 1990). During transport in the subsurface soil, infectious pathogenic organisms may be retained in the system, which is controlled by the soil moisture content, solution chemistry and pathogenic organism surface properties (Walker *et al.*, 1990; Guber *et al.*, 2005; Kim *et al.*, 2008b; Semenov *et al.*, 2009). During animal waste land applications, in situ colloids could also be mobilized, which may also affect infectious pathogenic organism retention and transport.

The aim of this study was to investigate the transport of infectious pathogenic organisms during animal waste land application practices. In our prior experiments, we have compared the surface properties and transport of *E. coli* O157:H7 and *E. coli* HB 101 and found not much difference. Therefore, we used *E. coli* HB 101 as the model strain in this research. In order for them to be easily identified and quantified, *E. coli* HB 101 was incorporated with green fluorescent protein genes. Colloid release and *E. coli* breakthrough were simulated using an implicit, finite-difference scheme with colloid release rate coefficient and *E. coli* deposition rate coefficient as constant, linear and exponential functions of the soil depth. The simulated results demonstrated that transport parameters were not consistent along the depth of the soil profile. The results of this research provided guidelines for animal waste land applications to avoid causing unintended harm to the environment.

MATERIALS AND METHOD

Bacterial Strains

Escherichia coli HB101 was obtained from ATCC (No. 33694) and was incorporated with green fluorescent protein (GFP) genes in order for them to be easily identified and quantified (Noah *et al.*, 2005). *Escherichia coli* was transformed with plasmid pGFP (cDNA vector, Clontech) according to the following protocol. A single colony of *E. coli* was grown on Luria-Bertani (LB) medium overnight at 37°C to mid log phase. The harvested bacteria were chilled for

15 min on ice and washed twice with ice-cold water. These bacteria were then mixed with pGFP (0.5 μg) in a 0.2-cm cuvette and electroporated with a Bio-Rad Gene Pulser at 2.5 kV, 25 μF and 200 Ω . After that, the bacteria were added to 1 ml of SOC Medium (2% Tryptone, 0.5% Yeast Extract, 10 mM NaCl, 10mM MgSO_4 , 10mM MgCl_2) and incubated with moderate shaking for 90 min at 37°C. The transformed culture was then plated onto LB agar plates with ampicillin (50 $\mu\text{g}/\text{ml}$) for selection. Prior research has demonstrated no differences in growth kinetics and other properties between these modified strains and the parental strains (Clegg *et al.*, 1996). After growth in LB broth at 37°C until late logarithmic phase in the presence of 50 $\mu\text{g}/\text{ml}$ ampicillin, *E. coli* strains bearing pGFP were collected by centrifuging at $10,000 \times g$ for 10 min. After washed twice with a sterilized buffer solution (potassium phosphate monobasic-sodium hydroxide buffer, Fisher Scientific, Pittsburgh, PA), they were re-suspended in sterilized nano-pure de-ionized water (Barnstead, Dubuque, IA) in the presence of 50 $\mu\text{g}/\text{ml}$ ampicillin to make a bacterial suspension. The bacterial concentration was maintained at 10^8 cells/ml as predetermined by ATP assay (Chen & Strevett 2001), which was used as the cell stock solution for the column experiments. The size of *E. coli* was measured using a Malvern Zetasizer 3000 Hsa (Malvern Instrument Ltd., Malvern, Worcs, UK) as described by Meinders *et al.* (1995), which were $1.01 \pm 0.04 \mu\text{m}$. ζ -potential of *E. coli* was quantified from their electrophoretic mobility by dynamic light scanning (Zetasizer 3000HAS, Malvern Instruments Ltd., Malvern, UK), and was determined to be $-10.6 \pm 0.4 \text{ mV}$.

Column Experiments

The soil used in this research was collected from Florida A&M University's agricultural research and extension field facilities located in Quincy, FL. Soil samples were collected up to 3 feet below the surface. The collected soil samples were immediately placed in a Styrofoam cooler and sealed and delivered to the laboratory. The soil samples were analyzed immediately after transported to the laboratory.

The results showed that the soil of this field had a pH between 6.0 and 7.2 and was strongly humic with humus content between 3.5 and 7%. The soil varied slightly in soil types: 40% as clay soil, 30% sandy clay, and 30% highly clayey sand, thus representing the variety of soil types in south region of America. A sieve analysis was performed to characterize the soil size distribution. Briefly, 600 ~ 700 g soil was weighed and placed in a drying oven for approximately 10 days at 30°C. After the samples were determined to be thoroughly dry, the dry weight was recorded. During

drying, all samples were broken up with a pestle and mortar. A stack of sieves was arranged from top to bottom in the respective order of decreasing sieve size openings, i.e. sieve number 4, 10, 20, 40, 60, 100, 140, and 200. A pan was placed after the 200 sieve. The dry soil samples were placed on a sieve shaker for 15 minutes. The total weight of the soil samples retained on each sieve was then determined.

Colloid release and *E. coli* transport were evaluated in intact soil columns collected from the same site as described above. The columns (10.0-cm ID \times 60.0-cm length) were vertically oriented with three tensiometers mounted evenly along the length of the columns. For each run of the column experiments, 1500 ml stock *E. coli* solution was applied using a sprinkler from the top by a peristaltic pump (Masterflex, Cole-Parmer, Vernon Hills, IL) at an irrigation rate of 100 ml/min. In situ colloids were consequently mobilized. After 1500 ml of *E. coli* solution was eluted, the column was continuously flushed with the sterilized nano-pure de-ionized water at the same irrigation rate until *E. coli* was completely eluted.

The elution was collected by a fraction collector and the colloid concentration was measured using a spectrophotometer against a calibration curve generated using the in situ colloid as a reference. *Escherichia coli* concentrations were quantified by the spread-plating procedure in terms of number of colony forming units (CFU). CFU formation on LB agar plates in the presence of 50 $\mu\text{g}/\text{ml}$ ampicillin after overnight incubation (24 hrs) at 37°C were counted under a UV lamp (365 nm).

During the experiments, matric potential within the soil was monitored and recorded using a Campbell Scientific CR-7X datalogger (Campbell Scientific, Inc.). Using the matric potential information, water content was quantified by fitting the van Genuchten equation (Toride, 1995):

$$S_e = [1 + (\alpha h)^n]^{(1/n-1)} \quad (1)$$

where S_e is the effective saturation (-); α is the inverse of the air-entry potential (cm^{-1}); h is the matric potential ($\text{cm-H}_2\text{O}$); and n is the parameter related to pore size distribution (-). Using pressure-plate measurements, α and n were determined to be 0.025 cm^{-1} and 0.177 and θ_s and θ_r were found to be 0.389 and 0.058 respectively. S_e is related to water volumetric content as follows (Toride, 1995):

$$S_e = \frac{\theta - \theta_r}{\theta_s - \theta_r} \quad (2)$$

where θ is the volumetric water content (cm^3/cm^3); θ_r is the residual water content (cm^3/cm^3); and θ_s is the saturated water content (cm^3/cm^3).

Colloid release was controlled by a kinetic desorption and was described by (Bradford *et al.*, 2002; Lenhart & Saiers 2002; Bradford *et al.*, 2003; Chen & Flury 2005):

$$\frac{\partial C}{\partial t} + \frac{\rho}{\theta} \frac{\partial S}{\partial t} = \frac{\partial}{\partial z} \left[D_z \frac{\partial C}{\partial z} \right] - \frac{J_w}{\theta} \frac{\partial C}{\partial z} \quad (3)$$

$$\frac{\partial S}{\partial t} = -\beta S \quad (4)$$

where C is the colloid concentration in the liquid phase (g/m^3); S is the colloid concentration on the sediments (mg/g); t is time (min); D_z is the apparent dispersion coefficient (m^2/s); ρ is the bulk density (g/m^3), J_w is the specific flow rate, i.e., Darcian fluid flux; z is the coordinate parallel to the flow (cm); and β is the first-order colloid release rate coefficient (min^{-1}). For colloid release, a constant flux was used for the upper boundary, i.e., $J_w C(0, t) = 0$, and a zero gradient was assumed for the lower boundary, i.e., $\theta D_z \partial C / \partial z = 0$. The initial conditions for colloid release were $C(x, 0) = 0$ and $S(x, 0) = S_0$. For matric potential, J_w was used for the upper boundary and a constant potential of $-10 \text{ cm-H}_2\text{O}$ was set for all times as the bottom boundary condition. For colloid release simulations, the initial colloid source S_0 for each breakthrough curve was obtained by integrating the experimental breakthrough curves to obtain the total amount of colloids eluted.

E. coli transport encountered retention in the soil. For this research, a single sink term was used to account for *E. coli* retention during transport:

$$\frac{\partial}{\partial t} [\theta C^*] = \frac{\partial}{\partial z} \left[D_z \theta \frac{\partial C^*}{\partial z} \right] - \frac{\partial}{\partial z} [J_w C^*] - k_1 \theta C^* \quad (5)$$

where C^* is the *E. coli* concentration in the liquid phase (cells/m^3) and k_1 is the deposition rate coefficient accounting for *E. coli* retention. The colloid release and *E. coli* breakthrough curves were simulated against **Eqs (3-5)** using an implicit, finite-difference scheme. All the parameters were optimized by minimizing the sum of squared differences between observed and fitted concentrations using the nonlinear least-square method.

RESULTS AND DISCUSSION

Soil Characterization

Based on the sieving analysis, around 99.363% of the particles were found to be smaller than 0.425 mm, i.e., passing through the 40 sieve. Around 0.229% of the particles were found to be smaller than 0.075 mm, i.e., passing through the 200 sieve (**Fig. 1**).

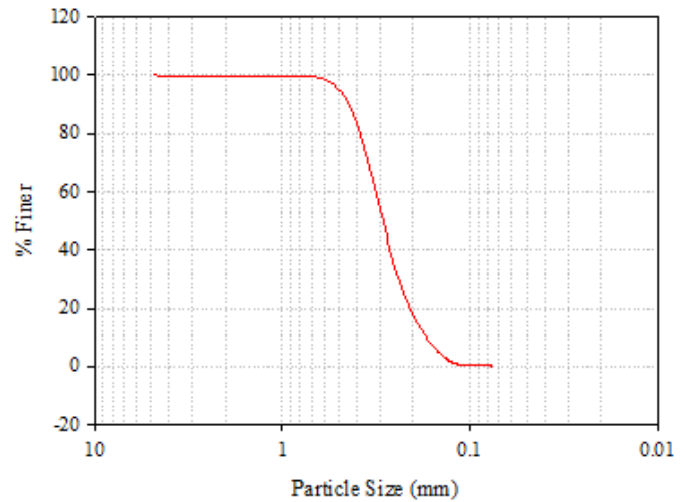


Fig. 1 Soil size distribution.

Matric Potential and Water Content

Before irrigation, the soil had an initial matric potential of -96 to -82 cm , corresponding to a water content of 0.19 to $0.238 \text{ cm}^3/\text{cm}^3$. Matric potential of the column decreased with the ongoing of irrigation until a steady state was reached, where matric potential remained constant for the sensors along the depth of the soil (**Fig. 2**). It took around one hour of irrigation before the steady-state flow phase and matric potentials were achieved. At the steady state, the matric potential was -28 cm on the top, -22 cm at the bottom and -25.5 cm in the middle of the column. Based on the van Genuchten equation, effective water saturation inside the column was calculated. Similar as matric potential, effective water saturation was not uniform along the depth of the soil (**Fig. 3**). Effective water saturation was 0.276 on the top, 0.342 at the bottom and 0.309 in the middle of the column, respectively. The soil had less effective water saturation on the top and higher effective water saturation at the bottom, indicating that water flow was controlled by the drainage at the bottom of the column. By plotting effective water saturation against matric potential, effective water saturation was found to have a sharp jump at matric potential of -25 cm in the middle of the column (**Fig. 4**). This was possibly owing to the heterogeneity of the soil and capillary force behavior in the soil. This phenomenon occurred before the steady state was reached. It was also demonstrated that the top, middle and bottom of the column had differences in effective water saturation with respect to matric potential. Since sandy soil and clayey soil had different water binding capacity, the differences in effective water saturation with respect to matric potential in **Fig. 4** was attributed to the uneven soil type distribution in the column.

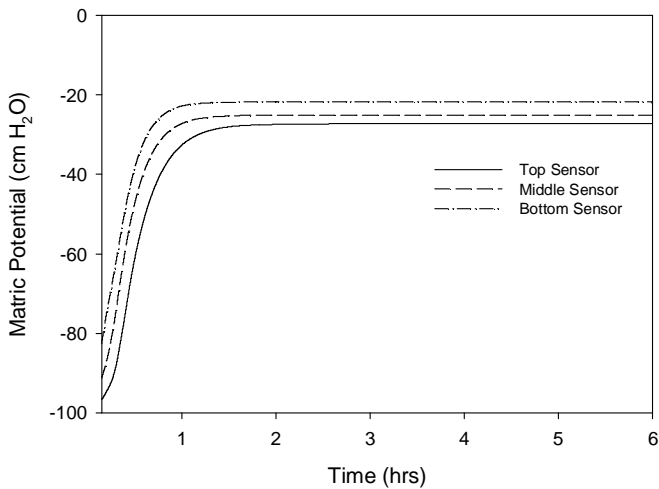


Fig. 2 Matrix potential as a function of time.

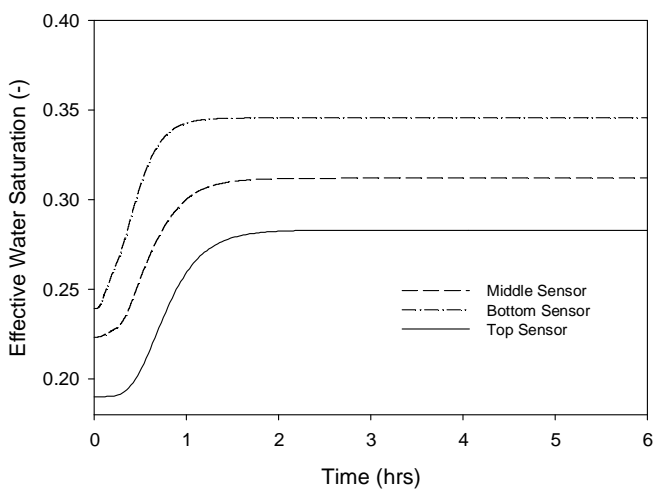


Fig. 3 Effective water saturation as a function of time.

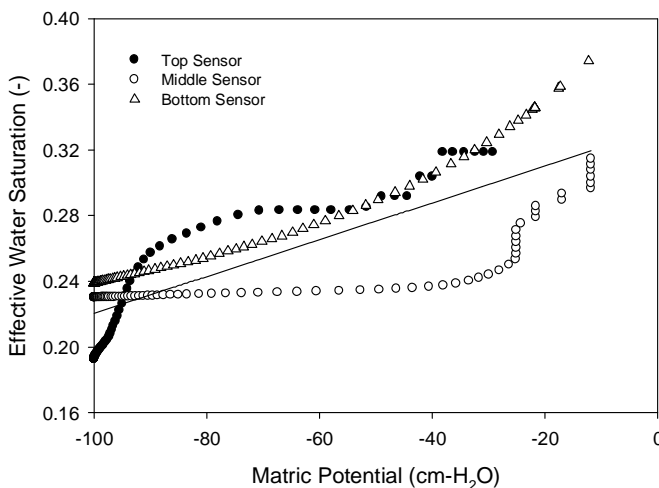


Fig. 4 Effective water saturation as a function of matric potential.

Since the effective water saturation was not even along the length of the column, the air-water interface had uneven distribution in the column. The air-water interface can be estimated from the pore size radius (Cary, 1994):

$$S_0 = \frac{\rho_0 g}{\alpha \gamma} \int_{\theta}^{\theta_0} \left[\left(\frac{\theta}{\theta_0} \right)^{\frac{n}{1-n}} - 1 \right]^{\frac{1}{n}} d\theta \quad (6)$$

where S_0 is the air-water interfacial area (cm^2/cm^3); ρ_0 is the water density (g/cm^3); g is the gravitational constant ($9.8 \text{ m}/\text{sec}^2$); γ is the water surface tension ($72.69 \text{ mJ}/\text{m}^2$ at 20°C); and θ_0 is the porous medium's volume fraction of pore space or porosity of the column. α and n are defined and reported previously. The air-water interfacial area increased with decreasing water saturation. At steady state, the effective water saturation ranging from 0.276 to 0.342 along the depth of the soil, corresponding to volumetric water content of 0.159 to 0.185. The air-water interfacial area was thus in the range from 136 to $125 \text{ cm}^2/\text{cm}^3$ from the top to the bottom of the column. Consequently, *E. coli* retention would be retained more on the top as compared to the bottom of the column.

Colloid Mobilization and *E. coli* Transport

When water front reached the bottom of the column, both in situ colloids and *E. coli* were observed in the effluent (Fig. 5). The colloid and *E. coli* breakthroughs coincided with the arrival of the infiltration front at the bottom of the column. The in situ colloid release and mobilization curves were characterized by a self-sharpening front, which became broader and diffuser at the elution limb. The long-lasting tails of the curves indicated kinetic-controlled colloid release from the soil in the column. By integrating the colloid breakthrough curves, the amount of in situ colloids released for the irrigation period of the experiment was used as the initial colloid source to obtain the colloid release rate coefficient. *Escherichia coli* breakthroughs were observed after colloid breakthroughs, which was less sharp in the self-sharpening front and more broad at the elution limb.

Mathematical models for colloid release and bacterial transport are usually based on the advection-dispersion equation (ADE) (Sen *et al.*, 2005). Currently, most of the available models are developed based on colloid release and transport observations. Though biological colloids (e.g., bacteria) and non-biological colloids (e.g., mineral colloids) differ in terms of potential physiological controls and polymeric material contributions, their transport behaviors in the environmental porous medium share important similarities. The most fundamental similarities are that they undergo deposition in the porous medium, which is usually described with the filtration theory and formulated as first-order kinetics. In these models, colloid release rate coefficient and bacterial deposition rate coefficient are usually assumed to be constant along

the depth of the soil, which is true under favorable attachment conditions (Or *et al.*, 2007; Kim *et al.*, 2008a). Consequently, bacterial concentration would display exponential decrease with the travel distance. However, a growing body of laboratory scale column experiments suggested that the retained bacterial profiles decayed nonexponentially under unfavorable attachment conditions, i.e., low ionic strength (Tufenkji *et al.*, 2003). Reported differences in deposition profile shape under unfavorable attachment conditions indicated apparent decrease in deposition rate coefficient with the transport distance (Li *et al.*, 2004; Bradford & Toride, 2007). In this research, colloid release and *E. coli* transport were simulated using an implicit, finite-difference scheme with colloid release rate coefficient and *E. coli* deposition rate coefficient as constant, linear and exponential functions of the soil depth, respectively (Fig. 4).

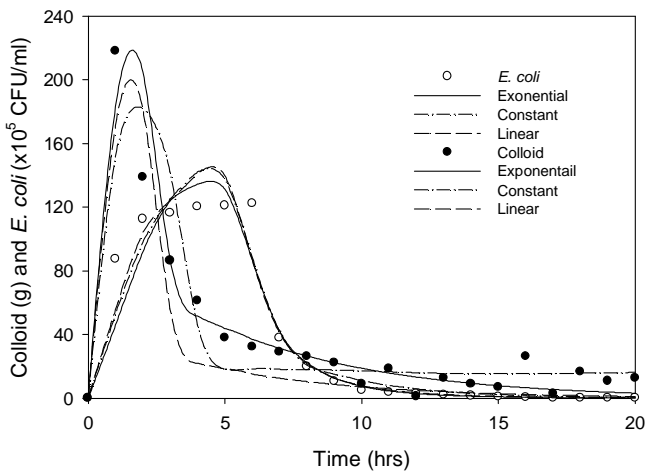


Fig. 5 Colloid release and *E. coli* breakthrough curves.

It seemed that exponential functions had the best fit against the colloid release and *E. coli* transport observations. The ADE with colloid release rate coefficient and *E. coli* deposition rate coefficient as constant and linear functions could capture the front part of the breakthrough curves well; however, the tail part did not fit well. These models predicted a less steep decline of the tail than was experimentally observed. It was expected the colloid release rate coefficient increased with water content and *E. coli* deposition rate coefficient decreased with water content. The simulated results were in consistence with above predictions (Figs 6 and 7). Since the column had higher water at the bottom than that of on the top, colloid release rate coefficient increased and *E. coli* deposition rate coefficient decreased along the depth of the soil column.

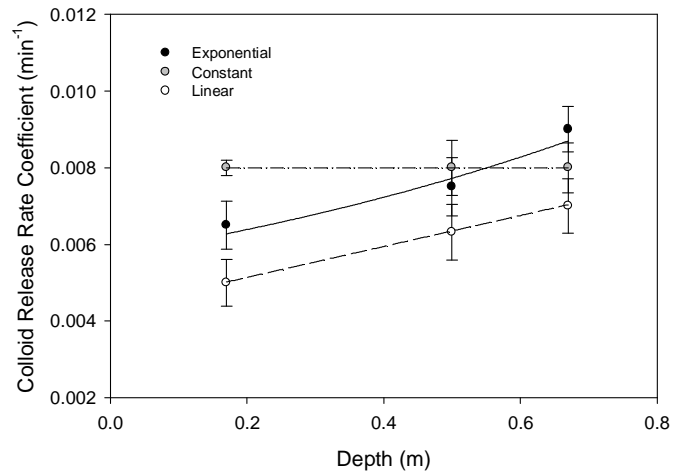


Fig. 6 Colloid release rate coefficient as a function of soil depth.

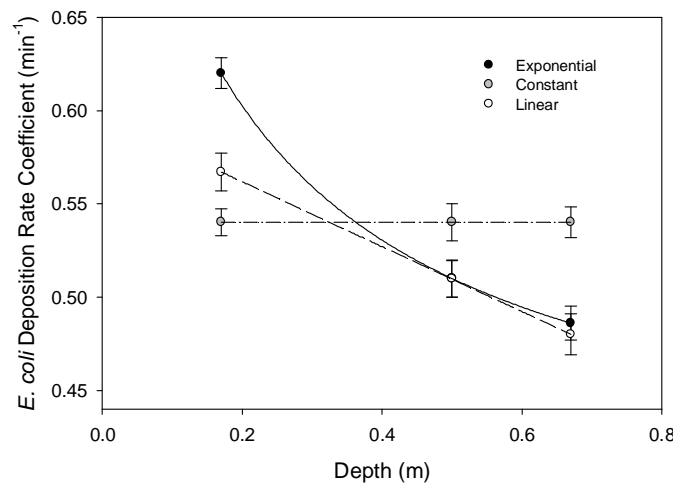


Fig. 7 *E. coli* deposition rate coefficient as a function of soil depth.

Colloids were retained in the porous media by capillary forces. With the increase of water content, capillary forces dropped and colloids were released accordingly. However, during colloid transport, colloids suffered from deposition owing to interactions and physical constraints of the air-water interface. For colloids in the pore system, release was dominating over deposition. *Escherichia coli* was introduced to the pore system. Consequently, deposition was the dominating process during its transport. Therefore, colloid release as a function of soil depth was attributed to water content and *E. coli* deposition was attributed to the air-water interface. Along the depth of the soil, the air-water interface decreased owing to the increase of water content. Accordingly, *E. coli* should have smaller deposition rate coefficient. In addition, decreased *E. coli* deposition might also be resulted from the elution of the in situ colloids. In other words, the mobilization of in situ colloids might enhance bacterial transport.

IMPLEMENTATION

All aspects of animal waste management are being explored to help farmers and local decision makers utilize the nutrient resources available in animal manure as an economic advantage in crop production while remaining environmentally sustainable in the long-term. Researchers have been working to design, improve, and test animal waste best management practices (BMPs) to prevent pathogenic bacteria from entering surface and groundwater. From this research, it was concluded that both in situ colloid release and pathogen transport were a function of soil depth. This research provides a framework for the assessment or evaluation of pathogenic bacterial spreading in agricultural fields. By properly managing the irrigation rate of animal waste agricultural applications, it is potentially possible to increase the propensity of pathogenic bacteria in the subsurface soil and protect the groundwater quality. Results of this proposed research will be useful for long-term animal waste field applications — a powerful means of nutrient recycling.

Acknowledgment The work was supported by the National Research Initiative of the USDA Cooperative State Research, Education and Extension Service, Grant No. 2007-35102-18111 to Florida A&M University.

REFERENCES

- Al-Sa'ed, R. (2007) Pathogens assessment in reclaimed effluent used for industrial crops irrigation. *Int. J. Environ. Res. Public Health* **4**(1), 68–75.
- Benckiser, G. & Simarmata, T. (1994) Environmental impact of fertilizing soils by using sewage and animal wastes. *Fertil. Res.* **37**(1), 1–22.
- Bradford, S.A., Simunek, J., Bettahar, M., Van Genuchten, M.T. & Yates, S.R. (2003) Modeling colloid attachment, straining, and exclusion in saturated porous media. *Environ. Sci. Technol.* **37**(10), 2242–2250.
- Bradford, S. A. & Toride, N. (2007) A stochastic model for colloid transport and deposition. *J. Environ. Qual.* **36**(5), 1346–1356.
- Bradford, S.A. Yates, S.R., Bettahar, M. & Simunek, J. (2002) Physical factors affecting the transport and fate of colloids in saturated porous media. *Water Res. Res.* **38**(12), 1327–1339.
- Brannan, K.M., Mostaghimi, S., McClellan, P.W. & Inamdar, S. (2000) Animal waste BMP impacts on sediment and nutrient losses in runoff from the Owl Run watershed. *Trans. ASAE* **43**(5): 1155–1166.
- Brenner, K. P. Scarpino, P.V. & Clark, C.S. (1988) Animal viruses, coliphages, and bacteria in aerosols and wastewater at a spray irrigation site. *Appl. Environ. Microbiol.* **54**(2), 409–415.
- Cary, J.W. (1994) Estimating the surface area of fluid-phase interfaces in porous media. *J. Contam. Hydrol.* **15**(4), 243–248.
- Chen, G. & Flury, M. (2005) Retention of mineral colloids in unsaturated porous media as related to their surface properties. *Colloid Surface A.* **256**(2–3), 207–216.
- Chen, G. & Strevett, K.A. (2001) Impact of surface thermodynamics on bacterial transport. *Environ. Microbiol.* **3**(4), 237–245.
- Clegg, C. D. Vanelas, J. D. Anderson, J. M. & LappinScott, H. M. (1996) Survival of parental and genetically modified derivatives of a soil isolated *Pseudomonas fluorescens* under nutrient-limiting conditions. *J. Appl. Bacteriol.* **81**(1), 19–26.
- Franco, A., Schuhmacher, M., Roca, E. & Luis Domingo, J. (2006) Application of cattle manure as fertilizer in pastureland: estimating the incremental risk due to metal accumulation employing a multicompartment model. *Environ. Int.* **32**(6), 724–732.
- Gerba, C.P. & Smith Jr., J.E., (2005) Sources of pathogenic microorganisms and their fate during land application of wastes. *J. Environ. Qual.* **34**(1), 42–48.
- Guber, A.K. Shelton, D.R. & Pachepsky, Y.A. (2005) Transport and retention of manure-borne coliforms in soil. *Vadose Zone J.* **4**(3), 828–837.
- Haapapuro, E.R., Barnard, N.D. & Simon, M. (1997) Review of animal waste used as livestock feed: dangers to human health. *Prev. Med.* **26**(5), 599–602.
- Hammond, R.C. (1972) Animal waste: a new problem. *J. Am. Vet. Med. Assoc.* **161**(11), 1322–1324.
- Irino, K. Vaz, T.M. Kato, M.A. Naves, Z.V. Lara, R.R. Marco, M.E. Rocha, M. M. Moreira, T. P. Gomes, T. A. & Guth, B. E. (2002) O157:H7 Shiga toxin-producing *Escherichia coli* strains associated with sporadic cases of diarrhea in Sao Paulo, Brazil. *Emerg. Infect. Dis.* **8**(4), 446–447.
- Jay, M.T. Cooley, M. Carychao, D. Wiscomb, G.W. Sweitzer, R.A. Crawford-Miksza, L., Farrar, J.A., Lau, D.K., O'Connell, J., Millington, A., Asmundson, R.V., Atwill, E.R. & Mandrell, R.E. (2007) *Escherichia coli* O157:H7 in feral swine near spinach fields and cattle, central California coast. *Emerg. Infect. Dis.* **13**(12), 1908–1911.
- Kim, M.K., Kim, S.B. & Park, S.J. (2008a) Bacteria transport in an unsaturated porous media: incorporation of air-water interface area model into transport modelling. *Hydrol. Process* **22**(13), 2370–2376.
- Kim, S.B., Park, S.J., Lee, C.G. & Kim, H.C. (2008b) Transport and retention of *Escherichia coli* in a mixture of quartz, Al-coated and Fe-coated sands. *Hydrol. Process* **22**(18), 3856–3863.
- Krauss, A.J. (2003) Waste management: small animal practice. *J. Am. Vet. Med. Assoc.* **223**(1), 53–54.
- Leclerc, H. Schwartzbrod, L. & Dei-Cas, E. (2002) Microbial agents associated with waterborne diseases. *Crit. Rev. Microbiol.* **28**(4), 371–409.
- Lenhart, J. J. & Saiers, J. E. (2002) Transport of silica colloids through unsaturated porous media: experimental results and model comparisons. *Environ. Sci. Technol.* **36**(4), 769–777.
- Li, X.Q., Scheibe, T.D. & Johnson, W.P. (2004) Apparent decreases in colloid deposition rate coefficients with distance of transport under unfavorable deposition conditions: a general phenomenon. *Environ. Sci. Technol.* **38**(21), 5616–5625.
- Mcgarvey, J.A. Miller, W.G. Sanchez, S. & Stanker, L. (2004) Identification of bacterial populations in dairy wastewaters by use of 16S rRNA gene sequences and other genetic markers. *Appl. Environ. Microbiol.* **70**(7), 4267–4275.
- Meinders, J.M. Vandermei, H.C. & Busscher, H.J. (1995) Deposition efficiency and reversibility of bacterial adhesion under flow. *J. Colloid Interf. Sci.* **176**(2), 329–341.
- Noah, C. W. Shaw, C. I. Ikeda, J. S. Kreuzer, K. S. & Sofos, J. N. (2005) Development of green fluorescent protein-expressing bacterial strains and evaluation for potential use as positive controls in sample analyses. *J. Food Prot.* **68**(4): 680–686.
- Or, D., Smets, B.F., Wraith, J.M., Dechesne, A. & Friedman, S.P. (2007) Physical constraints affecting bacterial habitats and activity in unsaturated porous media: a review. *Adv. Water Res.* **30**(6–7), 1505–1527.
- Pesaro, F. Sorg, I. & Metzler, A. (1995) In situ inactivation of animal viruses and a coliphage in nonaerated liquid and

- semiliquid animal wastes. *Appl. Environ. Microbiol.* **61**(1), 92–97.
- Schets, F. M., Van Wijnen, J.H., Schijven, J.F., Schoon, H. & De Roda Husman, A. M. (2008) Monitoring of waterborne pathogens in surface waters in amsterdam, the Netherlands, and the potential health risk associated with exposure to cryptosporidium and giardia in these waters. *Appl. Environ. Microbiol.* **74**(7), 2069–2078.
- Semenov, A. V. Van Overbeek, L. & Van Bruggen, A. H. (2009) Percolation and survival of *Escherichia coli* O157:H7 and *Salmonella enterica* serovar Typhimurium in soil amended with contaminated dairy manure or slurry. *Appl. Environ. Microbiol.* **75**(10): ,3206–3215.
- Sen, T.K., Das, D., Khilar, K.C. & Suraishkumar, G.K. (2005) Bacterial transport in porous media: New aspects of the mathematical model. *Colloid Surface A.* **260**(1–3), 53–62.
- Toride, N.L., Van Genuchten, F.J. (1995) *The CXTFIT Code for Estimating Transport Parameters from Laboratory or Field Experiments, Version 2.1.* Riverside, CA: U.S. Salinity Laboratory.
- Tufenkji, N., Redman, J.A. & Elimelech, M. (2003) Interpreting deposition patterns of microbial particles in laboratory-scale column experiments. *Environ. Sci. Technol.* **37**(3), 616–623.
- Walker, S.E., Mostaghimi, S., Dillaha, T.A. & Woeste, F.E. (1990) Modeling animal waste management practices: impacts on bacteria levels in runoff from agricultural lands. *Trans. ASAE* **33**(3), 807–817.
- Yan, T. & Sadowsky, M.J. (2007) Determining sources of fecal bacteria in waterways. *Environ. Monit. Assess.* **129**(1–3), 97–106.